Development of tolerance to bedaquiline by overexpression of trypanosomal acetate: succinate CoA transferase in *Mycobacterium smegmatis*

Check for updates

Gloria Mavinga Bundutidi[1,2,3,4,5], Kota Mochizuki [4,6], Yuichi Matsuo[7,8], Mizuki Hayashishita[7], Takaya Sakura[3,7,9], Yuri Ando[10], Gregory Murray Cook [11,12], Acharjee Rajib[3,7,9], Frédéric Bringaud [13], Michael Boshart [14], Shinjiro Hamano [1,2], Masakazu Sekijima [15], Kenji Hirayama[4,7], Kiyoshi Kita[7,9,16] & Daniel Ken Inaoka [3,7,9,16] ✉

The F-type ATP synthase inhibitor bedaquiline (BDQ) is a potent inhibitor of mycobacterial growth and this inhibition cannot be rescued by fermentable carbon sources that would supply ATP by an alternative pathway (substrate level phosphorylation). To gain mechanistic insight into this phenomenon, we employed a metabolic engineering approach. We introduced into *Mycobacterium smegmatis* an alternative ATP production pathway by substrate-level phosphorylation, specifically through overexpression of trypanosomal acetate:succinate co-enzyme A (CoA) transferase (ASCT). Intriguingly, the overexpression of ASCT partially restored intracellular ATP levels and resulted in acquired tolerance to BDQ growth inhibition at low, but not high concentrations of BDQ. These results implicate intracellular ATP levels in modulating the growth inhibitory activity of BDQ at low concentrations. These findings shed light on the intricate interplay between BDQ and mycobacterial energy metabolism, while also providing a novel tool for the development of next-generation ATP synthase-specific inhibitors targeting mycobacteria.

Tuberculosis (TB) has emerged as a significant global health concern, currently ranking as the 13th leading cause of mortality, and standing as the second-most-lethal infectious disease after Coronavirus Disease 2019 (COVID-19)[1]. The World Health Organisation (WHO) reported 10.6 million TB cases in 2021, involving 6 million men, 3.4 million women, and 1.2 million children[1]. Achieving global control targets in combatting this disease was projected to require (by 2022) an annual expenditure of USD 13 billion for TB prevention, diagnosis, treatment, and care[2]. The emergence of multidrug-resistant TB (MDR-TB) and extensively drug-resistant TB (XDR-TB) presents a formidable challenge to existing TB control programmes[1,3]. Without effective new anti-TB drugs, MDR-TB and XDR-TB pose significant global health threats. Consequently, there is an urgent need to identify novel and potent TB drugs that can offer effective treatment[4].

Oxidative phosphorylation (OXPHOS), represents a prominent metabolic pathway in mycobacteria, playing a pivotal role in both energy production and bacterial proliferation[5,6]. Within the OXPHOS pathway, protons (H$^+$) are translocated, creating an electrochemical gradient across the inner membrane. The resulting proton motive force (PMF) drives the synthesis of adenosine triphosphate (ATP) by the ATP synthase; the resulting ATP serves as a primary energy source for mycobacteria[6,7]. The utility of targeting the OXPHOS pathway is demonstrated by the activity of compound classes that include diarylquinoline and benzothiazinone antimicrobials, exposure to which induces a swift decrease in bacterial viability[8,9].

Bedaquiline (BDQ), a diarylquinoline drug, represents the first TB treatment with a novel mechanism of action that has been approved by the US Food and Drug Administration (FDA) in the past four decades[10,11]. BDQ inhibits the energy metabolism of mycobacterial species such as *Mycobacterium tuberculosis* and *M. smegmatis*. The latter, a non-pathogenic, rapidly proliferating organism, serves as a valuable surrogate for studying the energy metabolism and respiratory chain of mycobacteria. Compared to other mycobacteria, *M. smegmatis* provides ease of handling in an organism for which genomic data is available and in which essential genes are

conserved[12]. Moreover, the conservation of fundamental physiological pathways, versatile carbon source utilisation, comparable cell wall composition, and lipid metabolism in both *M. tuberculosis* and *M. smegmatis* have positioned the latter as a valuable asset in antimycobacterial drug discovery efforts[13].

BDQ exhibits multiple mechanisms of action at different concentrations. In the nanomolar range, it functions as an inhibitor of F-ATP synthase, selectively binding to the hydrophobic region of subunit *c* within the F_1F_O-ATP synthase complex. At micromolar concentrations, BDQ increases the oxygen consumption rate, thus apparently acting as an uncoupler[14–16]. However, despite BDQ's potent bactericidal effect[8,10,16], the precise mechanism by which the compound induces growth inhibition and cell death in mycobacteria, including *M. smegmatis*, remains unclear, although it likely involves multiple factors[17,18]. Furthermore, the treatment of MDR-TB presents significant challenges due to the notable side effects associated with BDQ and the emergence of BDQ-resistant strains[19,20]. Therefore, gaining a deeper understanding of the mechanism of action of BDQ would be of great value in the development of more potent compounds and/or derivatives capable of combating MDR-TB.

Several investigations have provided insights into the metabolic adaptations of mycobacteria treated with BDQ, suggesting a shift towards glycolysis as the primary ATP production pathway to compensate for reduced ATP levels[18,21]. However, an alternative line of research proposes that the energy obtained through substrate-level phosphorylation (SLPHOS) during glycolysis would be insufficient to meet the demands of bacterial growth, compromising long-term survival[22,23]. To address this discrepancy, one study employed simultaneous inhibition of both SLPHOS (via glycolysis disruption) and OXPHOS (using BDQ); under these conditions, *M. tuberculosis* was rapidly eliminated[17]. Therefore, we hypothesised that mycobacteria provided with an alternative source of ATP (via SLPHOS) would display reduced susceptibility to BDQ, perhaps even gaining resistance to BDQ.

Trypanosome parasites, specifically *Trypanosoma brucei* and *T. cruzi*, agents of African sleeping sickness and Chagas disease, respectively, utilize the acetate:succinate co-enzyme A (CoA) transferase/succinyl-CoA synthetase (ASCT/SCS) cycle to independently produce ATP, irrespective of oxygen and electrochemical gradient[24,25]. This cycle involves the utilisation of acetyl-CoA and succinate by ASCT to produce acetate and succinyl-CoA; the succinyl-CoA is then used by SCS to generate ATP while regenerating succinate and CoA[24]. In *T. brucei*, the ASCT/SCS cycle plays a significant role in conferring resistance to oligomycin A, a potent inhibitor of ATP synthase[26].

In the present study, we sought to understand the role of ATP in the antimycobacterial activity of BDQ. Here, we show that metabolic engineering of the trypanosomal ASCT/SCS cycle in *M. smegmatis* alleviates the bacteriostatic effect of BDQ at low doses by maintaining higher intracellular ATP levels than the control. However, at higher doses of BDQ, the trypanosomal ASCT/SCS cycle cannot rescue ATP levels and growth.

Results

We have previously demonstrated the importance of the ASCT/SCS cycle in *T. brucei* under OXPHOS-deficient conditions[26,27]. Importantly, we have shown that *T. brucei* ASCT/SCS cycle exhibits a higher turnover number (k_{cat}) than that of the ATP synthases found in yeast and bacteria[27]. This property makes it a potential tool to study the contribution of ATP in the mechanism of action of BDQ by metabolic engineering the trypanosomal ASCT/SCS cycle in mycobacteria.

Overexpression of trypanosomal ASCT in *M. smegmatis*

To assess the effects of additional ATP production on the mycobacterial activity of BDQ, *T. cruzi* ASCT (TcASCT) and *T. brucei* ASCT (TbASCT) were first expressed in *M. smegmatis* using the pYUB28b vector[28]. The expression of functional TcASCT and TbASCT was confirmed using the previously established method whereby the ASCT/SCS cycle was reconstituted using mycobacterial cells lysates[27]. Notably, TcASCT demonstrated a higher specific activity (1.065 ± 0.025 µmol/min/mg protein, mean ± SD) than did TbASCT (0.675 ± 0.046 µmol/min/mg protein). In contrast, lysates of the control strain (*M. smegmatis* transfected with the empty vector) exhibited no detectable activity (Fig. 1a).

ASCT expression in *M. smegmatis* was further confirmed by western blot analysis, which revealed the presence of protein bands at the expected masses of 52 kDa (Fig. 1b). The apparent sizes of the TbASCT and TcASCT proteins in the mycobacterial cell lysates were similar to those of the respective purified recombinant proteins, confirming the successful
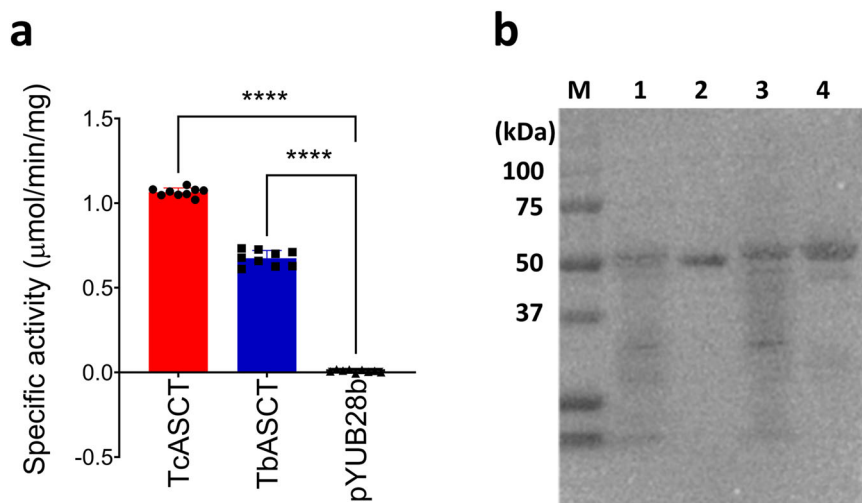
Fig. 1 | Analysis of transgenic *M. smegmatis* expressing trypanosomal ASCT.
a ASCT activity was measured spectrophotometrically in 50 mM Tris–HCl (pH 7.4) at 37 °C using the mycobacterial cell lysates. Reactions were initiated by the addition of succinate, and progress was monitored by following the production of 5-thio-2-nitrobenzoic acid, as detected by absorbance at 412 nm. Data represent the specific activity of each strain and are expressed as mean ± SD from three independent experiments. Activities were compared among lysates from *M. smegmatis* expressing TcASCT or TbASCT, as well as from a control strain harbouring the empty plasmid (pYUB28b). Comparisons were performed using two-tailed one-way ANOVA with post hoc Tukey's multiple comparisons tests, as indicated. ****$p < 0.0001$.
b Overexpression of trypanosomal ASCT was confirmed by western blotting analysis using anti-ASCT as the primary antibody. Proteins corresponding to ASCT in the lysates ran as bands of sizes similar to those of the purified recombinant trypanosomal ASCTs. Lanes: M marker; 1: *M. smegmatis* TcASCT lysate; 2: recombinant TcASCT; 3: *M. smegmatis* TbASCT lysate; 4: recombinant TbASCT. Molecular weights (kDa) of the marker ladder are indicated to the left. Unedited Western blot picture is provided in Supplementary Data 1.

expression in *M. smegmatis* of both trypanosomal ASCT enzymes in the active form.

Biochemical characterisation of purified TcASCT

Previously, it was reported that the ASCT/SCS cycle in *T. brucei* functions optimally at 30 °C[27]. However, to the best of our knowledge, no prior investigations have explored TcASCT. The heightened specific activity observed in TcASCT expression within *M. smegmatis*, as demonstrated in Fig. 1a, underscores the critical necessity for further biochemical inquiries into TcASCT.

Hence, tag-free TcASCT lacking the mitochondrial targeting signal was successfully expressed in *Escherichia coli* BL21Star™(DE3) strain and purified to homogeneity. Under optimal conditions, bacterial growth in the main culture achieved a mean OD_{600} value of 10.4 across six flasks when cultured in Terrific Broth medium for 12 h at 20 °C. A total of 24.4 mg tag-free TcASCT was purified from 3.6 L of culture, with 39% recovery of total activity and specific activity of 108 μmol/min/mg protein, representing a 34-fold purification compared to the *E. coli* lysate. The results of the purification are summarised in Supplementary Table 1. The purity of TcASCT exceeded 95%, as judged by the SDS–PAGE gel. A band of the expected size was observed on the gel after protein staining, consistent with the predicted mass of 52 kDa for the tag-free TcASCT (Supplementary Fig. 1).

Purified recombinant tag-free TcASCT was characterised biochemically using the in vitro reconstituted ASCT/SCS cycle assay[27]. TcASCT activity exhibited a linear dose–response over a protein concentration range of 11.6–186 ng/mL in the assay mixture, with this curve exhibiting an R^2 value of 0.979. We, therefore, chose to conduct subsequent assays using an enzyme concentration of 100 ng/mL TcASCT. The optimal temperature (Fig. 2a) and pH (Fig. 2b) for the reaction were determined to be 37 °C and 7.0, respectively. The K_m values for acetyl-CoA and succinate were 0.089 and 4.87 mM, respectively (Supplementary Table 2 and Supplementary Fig. 2). At a high concentration of succinate, substrate inhibition was apparent, giving a K_i of 106 mM (Supplementary Fig. 2).

Mycobacterial expression of trypanosomal ASCT relieves growth inhibition by ATP synthase inhibitors

Mycobacteria strains expressing ASCT, as well as the control strain (carrying the empty vector) cultured in Luria-Bertani supplemented with 0.05% (v/v) Tween 80 (LBT) medium were exposed to either vehicle (DMSO) or various concentrations of BDQ (1, 3, 5, 7, and 9 ng/mL; which correspond to 1.8, 5.4, 9.0, 12.6, and 16.2 nM) near its EC_{50} value of 5 ng/mL (Supplementary Fig. 3). When *M. smegmatis* strains were cultured in the absence of BDQ (i.e., with DMSO), a statistically significant difference in the growth rate was observed among the ASCT-expressing and control strains (Fig. 3a). Similarly, at 1 ng/mL BDQ, growth rates of ASCT-expressing strains were faster than the control strain (Fig. 3b). Moreover, the impact of ASCT

expression on BDQ-treated mycobacteria became evident when the strains were exposed to concentrations of 3, 5, and 7 ng/mL BDQ (Fig. 3c–e, respectively). Although BDQ at these concentrations caused complete growth arrest in the control strain (empty vector), the strain expressing TcASCT (and, to a lesser extent, that expressing TbASCT) was able to sustain growth under the same conditions. However, at a higher concentration of BDQ (9 ng/mL), none of the recombinant mycobacteria were able to recover growth (Fig. 3f). Similar results were observed when these *M. smegmatis* strains were cultured on solid medium, where the expression of TcASCT allowed the mycobacteria to grow in the presence of BDQ at concentrations of up to 7 ng/mL (Supplementary Fig. 4). We conducted an additional experiment exploring the potential inhibitory effect of BDQ on ASCT. Even at a saturating concentration of BDQ (200 μM), no inhibition of TbASCT activity was observed (Supplementary Fig. 5).

Mycobacteria are known to exhibit metabolic flexibility, particularly when cultured in the presence of different carbon sources[21,29,30]. To determine the possible effect of carbon source on tolerance/resistance to BDQ, we investigated the impact of ASCT expression in *M. smegmatis* growing in the minimal medium supplemented with each of a range of fermentable (glucose and glycerol) and non-fermentable (malate, acetate, and succinate) carbon sources. The concentrations of these carbon sources were normalized by the number of carbons supplemented: 15 mM for C6 (glucose), 22.5 mM for C4 (malate and succinate), 30 mM for C3 (glycerol), and 45 mM for C2 (acetate). Notably, when cultured with each of these carbon sources in a minimal medium containing 0.1% DMSO (the vehicle for BDQ), no discernible difference in growth was observed among the ASCT-expressing and control strains. However, in the presence of BDQ, the expression of ASCT conferred benefits to mycobacteria (Fig. 4). The growth rate varied depending on the carbon source and glucose-growing cells expressing ASCT were particularly insensitive to inhibition by BDQ (Fig. 4, bottom panel). Surprisingly glycerol-grown cells exhibited the greatest sensitivity to BDQ. Taken together, these data infer that at low concentrations of BDQ, the major mechanism of action involves inhibition of F-ATP synthase leading to growth inhibition. This growth inhibition can be partially rescued by boosting SLPHOS through the ASCT/SCS cycle in *M. smegmatis*.

Previous work has demonstrated that BDQ causes cell death in a time-dependent manner[18]. Therefore, we next assessed the nature of growth recovery conferred by ASCT expression in BDQ-exposed *M. smegmatis*. For this experiment, each of the mycobacterial strains was cultured in 96-well plates containing LBT medium supplemented with various concentrations of BDQ; growth was assessed at 2, 3, and 5 days. On Day 2 (Fig. 5a), slight differences in GI_{50} were observed, such that the TcASCT-expressing strain exhibited higher values than the control strain (11.3 vs. 7.7 ng/mL, respectively). On Day 3, the GI_{50} of the control strain decreased to 6.4 ng/mL, while that of the TcASCT-expressing strain (10.1 ng/mL) remained similar to that

Fig. 2 | Determination of optimal temperature and pH for TcASCT activity. a The enzymatic assays to determine the optimal temperature were conducted in 100 mM Tris–HCl (pH 6.8). Reactions were initiated by the addition of succinate, and progress was monitored by following the production of NTB, as detected by absorbance at 412 nm. **b** Determinations of optimal buffer and pH conditions were conducted by assessing activity at 37 °C under the conditions described in (**a**). Data are presented as the mean ± SD of three biological replicates.
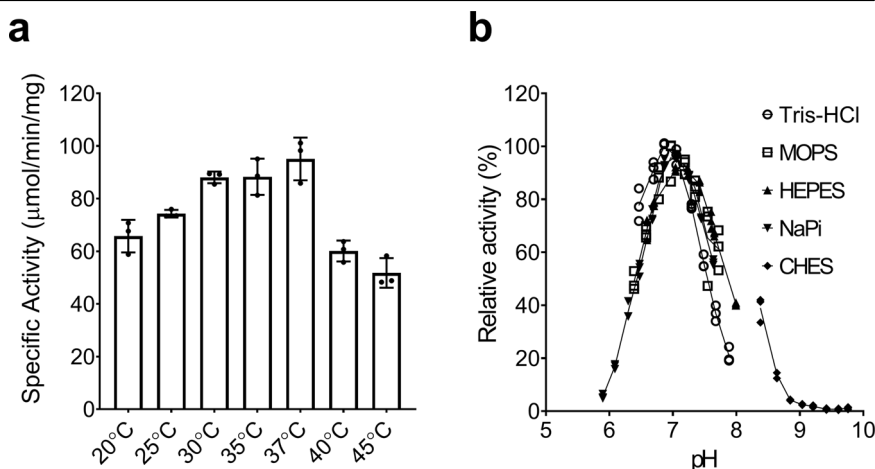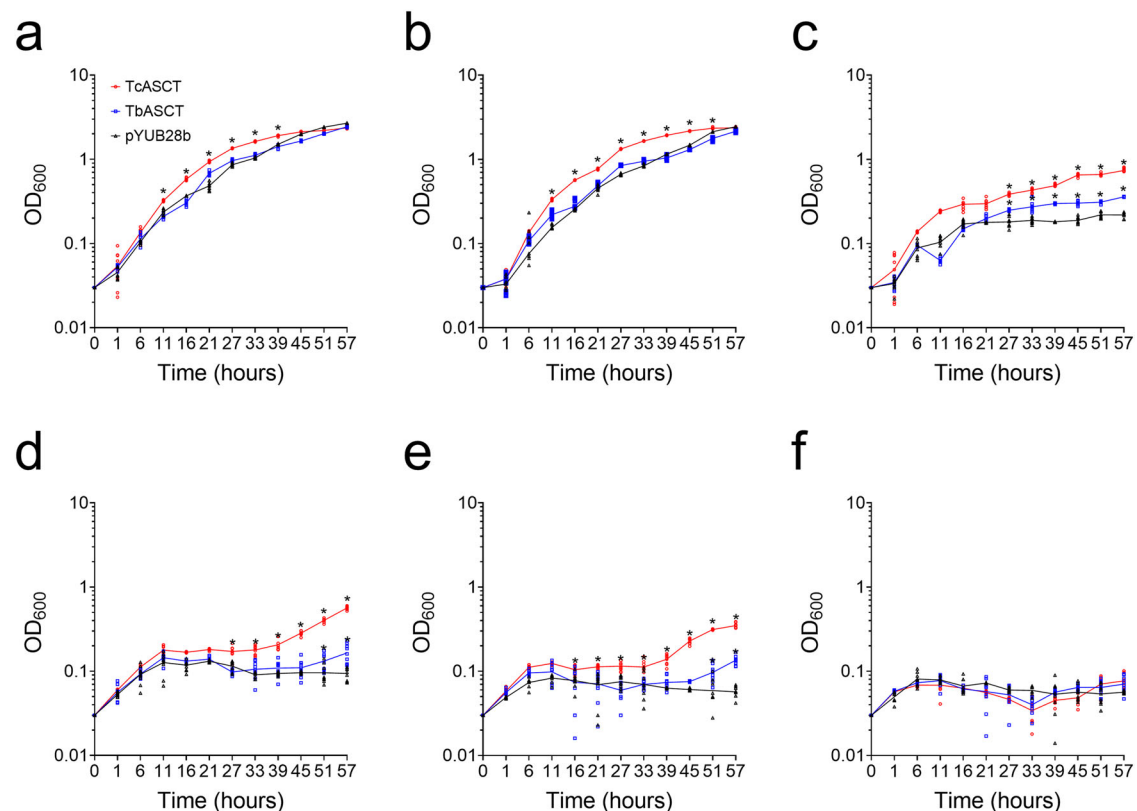
Fig. 3 | The expression of trypanosomal ASCT rescues the growth of *M. smegmatis* in the presence of up to 7 ng/mL BDQ. Growth (OD_{600}) of *M. smegmatis*-expressing TcASCT or TbASCT, as well as that of the control strain harbouring the empty vector (pYUB28b), were cultured in LBT medium in the presence of DMSO (the vehicle used for formulating BDQ) (**a**), 1 ng/mL BDQ (**b**), 3 ng/mL BDQ (**c**), 5 ng/mL BDQ (**d**), 7 ng/mL BDQ (**e**), and 9 ng/mL BDQ (**f**). Cells were initially cultured in an LBT medium until the exponential phase, then diluted into a fresh medium at an initial OD_{600} of 0.03, to which DMSO or BDQ at various concentrations was added. Bacterial growth was monitored by measuring the OD_{600} over time. Asterisks indicate data points showing statistically significant differences (Welch *t*-test, $p \leq 0.05$) in the ASCT strains compared to the control (pYUB28b). Data are presented as the mean ± SD for the results of experiments performed as three biological replicates.

observed on Day 2 (Fig. 5b). These differences in GI_{50} became more pronounced on Day 5, when the value for the control strain decreased to 3.6 ng/mL, while that of the TcASCT-expressing strain increased to 24.2 ng/mL (Fig. 5c). Similar patterns were observed for the TbASCT-expressing strain, with the GI_{50} exhibiting a gradual increase from 8.1 to 8.4–16.9 ng/mL on Days 2, 3, and 5, respectively (Fig. 5a–d). Notably, after 5 days of exposure to BDQ, the GI_{50} of the inhibitor for the TcASCT-expressing *M. smegmatis* was 7-fold that for the control strain. These findings highlighted the time-dependent nature of ASCT-mediated growth recovery in the presence of BDQ and provided further insights into the dynamics of the interaction between ASCT expression and BDQ-induced growth inhibition in *M. smegmatis*. Interestingly, the MIC observed by the resazurin microtiter assay (REMA) shifted from 30 to 100 ng/mL on day 5 for *M. smegmatis*-expressing TcASCT and TbASCT, whilst reducing approximately to 10 ng/mL for the control strain (Fig. 5c).

Expression of trypanosomal ASCT in *M. smegmatis* increases intracellular ATP levels in presence of ATP synthase inhibitors
Finally, we investigated whether the tolerance to BDQ seen in *M. smegmatis* expressing ASCT (Figs. 4 and 5) correlates with the intracellular level of ATP. We hypothesized that the SLPHOS activity provided by the engineered ASCT/SCS cycle is associated with the response to BDQ. For this experiment, we monitored the ATP levels of the transgenic mycobacteria cultured in the presence of various concentrations of BDQ. In control (empty vector) *M. smegmatis* strain, intracellular ATP levels and growth showed a noticeable decrease at BDQ concentrations as low as 1 ng/mL, with a more pronounced decline in growth and ATP at 3 ng/mL BDQ

(Fig. 6a, b). In contrast, *M. smegmatis* expressing either ASCT maintained intracellular ATP levels that were significantly higher than those of the control group, along with sustained mycobacterial growth, at 1 and 3 ng/mL BDQ. Although the overall growth was significant lower for all strains expressing ASCT at BDQ concentrations of 5 ng/mL, they still maintained higher intracellular ATP levels and growth compared to the control group. Consistent with previous findings, exposure to DMSO did not impact intracellular ATP levels, while exposure to 10 ng/mL BDQ resulted in large decreases in both the intracellular ATP levels and growth of all tested strains (Fig. 6a, b), independently of trypanosomal ASCT expression. To ensure the tolerance was not acquired by a specific class of compounds, we next tested if a different class of ATP synthase inhibitor would render the same phenotype observed for BDQ. For this, we used oligomycin A, which is a non-specific ATP synthase inhibitor, and as shown in Supplementary Fig. 6, strains expressing ASCT had higher levels of ATP and growth than the control group.

Discussion
Resistance to the F-type ATP synthase inhibitor BDQ, along with low safety margin, accentuates the need for ongoing research and development to identify new anti-TB drugs that target ATP production[31,32]. Such drug development requires a comprehensive understanding of the underlying mechanism of action of existing drugs. BDQ has been shown to inhibit F-ATP synthase function and decrease intracellular ATP levels. However, other studies have failed to detect a correlation between mycobacterial death and decreased intracellular ATP levels induced by starvation[33,34]. Therefore, the precise mode of action by which BDQ causes growth inhibition, even in
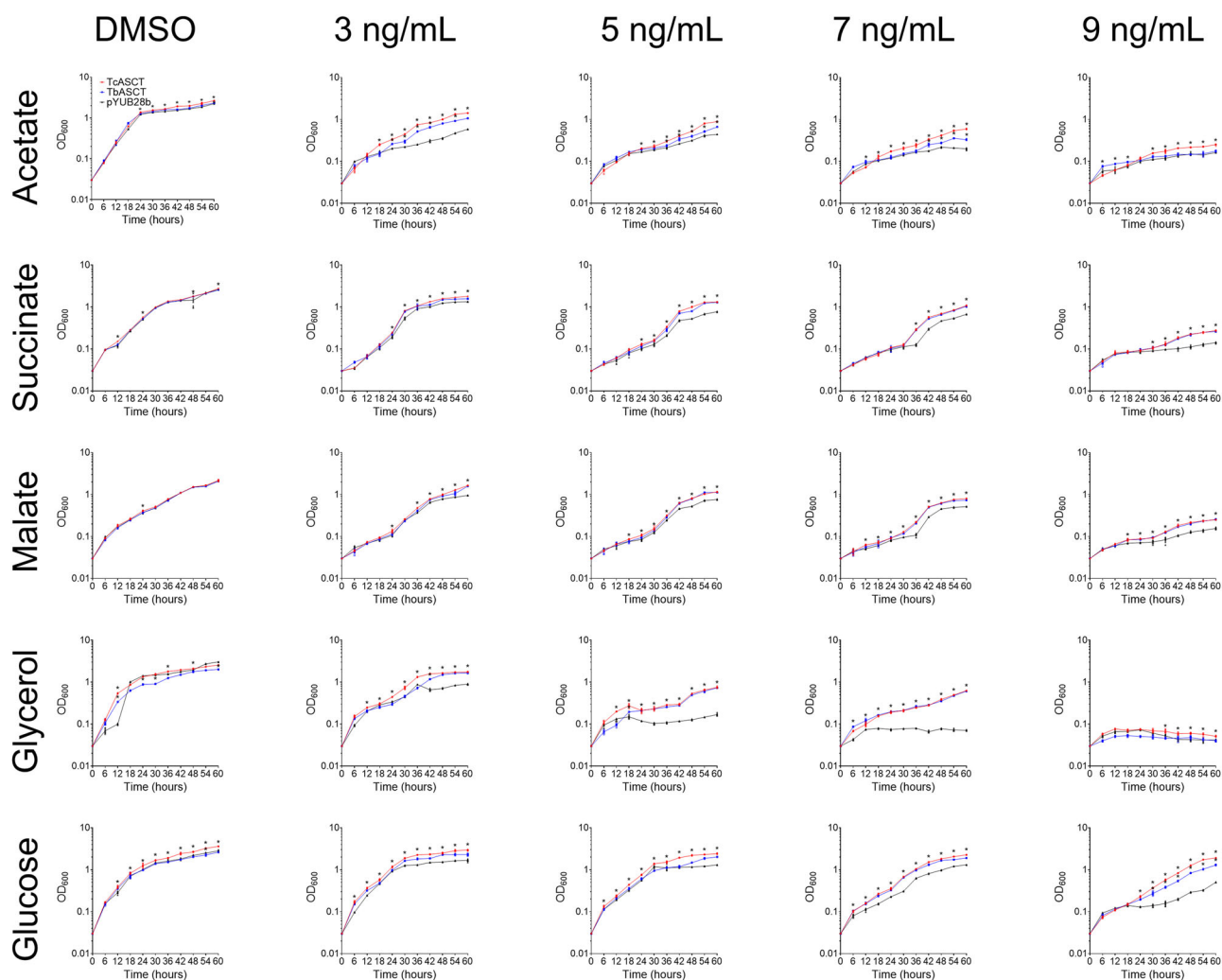
Fig. 4 | Effect of different carbon sources on BDQ-induced growth inhibition rescue by ASCT expression. The effects of ASCT on transgenic *M. smegmatis* treated with various concentrations of BDQ were investigated by culturing cells in minimal media (HdeB) supplemented with various carbon sources: 22.5 mM malate, 30 mM glycerol, 45 mM acetate, 22.5 mM succinate, or 15 mM glucose. Asterisks indicate statistically significant differences ($p \leq 0.05$, Welch's *t*-test) in ASCT strains compared to the control (pYUB28b). Results represent means ± SD from three biological replicates per experiment.

the presence of a fermentable carbon source that can provide ATP by substrate-level phosphorylation requires further investigation. We previously found that ASCT from *T. brucei* provides additional ATP when OXPHOS is inhibited[26,27]. Therefore, we hypothesised that overexpression of this enzyme in *M. smegmatis* would render this bacterium tolerant or resistant to BDQ if, indeed, mycobacterial growth was limited by ATP production. To investigate this further, both trypanosomal ASCTs were expressed as functional enzymes in *M. smegmatis*, with TcASCT exhibiting a higher specific activity than TbASCT. To better understand the enhanced specific activity of TcASCT in *M. smegmatis*, we conducted biochemical studies on purified ASCT from *T. cruzi*, which exhibited several similarities to the properties reported for TbASCT[27]. Kinetic parameters such as K_m and k_{cat} as well as the substrate specificity, were of the same order for the ASCTs from the two organisms. However, distinct biochemical features were found. In the previous work, we noted that the optimal temperature of TbASCT was 30 °C, and a sharp decrease in activity was seen at 37 °C[27]. In contrast, we found that TcASCT exhibited an optimal temperature of 37 °C and that the enzyme retained about 90% of enzymatic activity when tested at 30 °C. This finding suggests that the ASCT may be required for survival in both the mammalian host and the insect vector (kissing bug) of *T. cruzi*. This observation is consistent with the fact that de novo fatty acid biosynthesis is essential in all life-cycle stages of *T. cruzi*[27], and ASCT is known to be the sole source of acetate required for this pathway in trypanosomes via acetyl-CoA

synthase present in the cytosol. Thus, the difference observed between the lysates of strains expressing either of the two enzymes presumably reflects the fact that these experiments were performed at 37 °C, which is the optimal temperature for TcASCT activity and *M. smegmatis* growth.

As we hypothesised, the expression of trypanosomal ASCTs in *M. smegmatis* mitigated the inhibitory effect of BDQ on mycobacterial growth, specifically at low concentrations of BDQ. This result is consistent with the observation that in *T. brucei*, an active ASCT/SCS cycle is responsible for that organism's natural resistance to an ATP synthase inhibitor, oligomycin A[26,27]. In the case of *M. smegmatis* expressing TbASCT or TcASCT, it utilizes the endogenous SCS, consisting of SucC (Accession: ABK71969) and SucD (Accession: ABK72035) subunits, to complete the ASCT/SCS cycle. Therefore, the rate of ATP production by the ASCT/SCS cycle is limited by the expression level and activity of endogenous SCS in these strains. Consequently, one would expect a higher level of BDQ tolerance if ASCT is expressed in a strain where SCS is overexpressed.

We further observed that when *M. smegmatis* strains were exposed to higher concentrations of BDQ, the expression of ASCT was not sufficient to rescue the growth inhibition of BDQ. We postulate that higher concentrations of BDQ impede mycobacterial growth via severe depletion of intracellular ATP[18] that cannot be rescued by an alternative ATP source (e.g., SLPHOS from glycolysis). This finding reinforces the crucial role of OXPHOS in mycobacterial growth[23]. In contrast, in other microbes such as

Fig. 5 | ASCT expression in *M. smegmatis* decreases susceptibility to BDQ, an ATP synthase inhibitor, in a time-dependent manner. *M. smegmatis* strains expressing either ASCT, as well as the control strain harbouring the empty vector (pYUB28b), were cultured (in 96-well plates at 37 °C) in LBT medium containing various concentrations of BDQ. On Day 2 (**a**), Day 3 (**b**), and Day 5 (**c**) after the addition of BDQ, relative growth was assessed using a resazurin microtiter assay (REMA). The concentration of the compound that inhibit cell growth to 50% (GI$_{50}$) for each strain was determined and plotted against the respective time point (**d**). Data in (**b**) and (**c**) are presented as the mean ± SD for the results of experiments performed as two biological replicates.
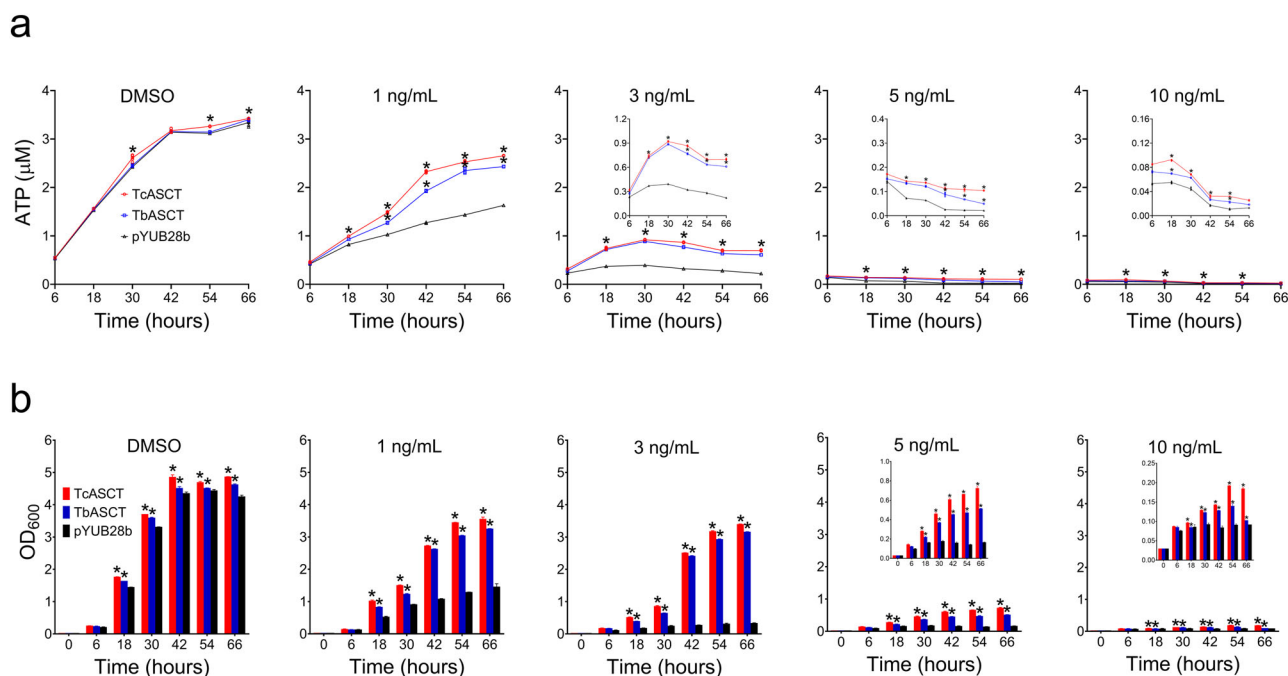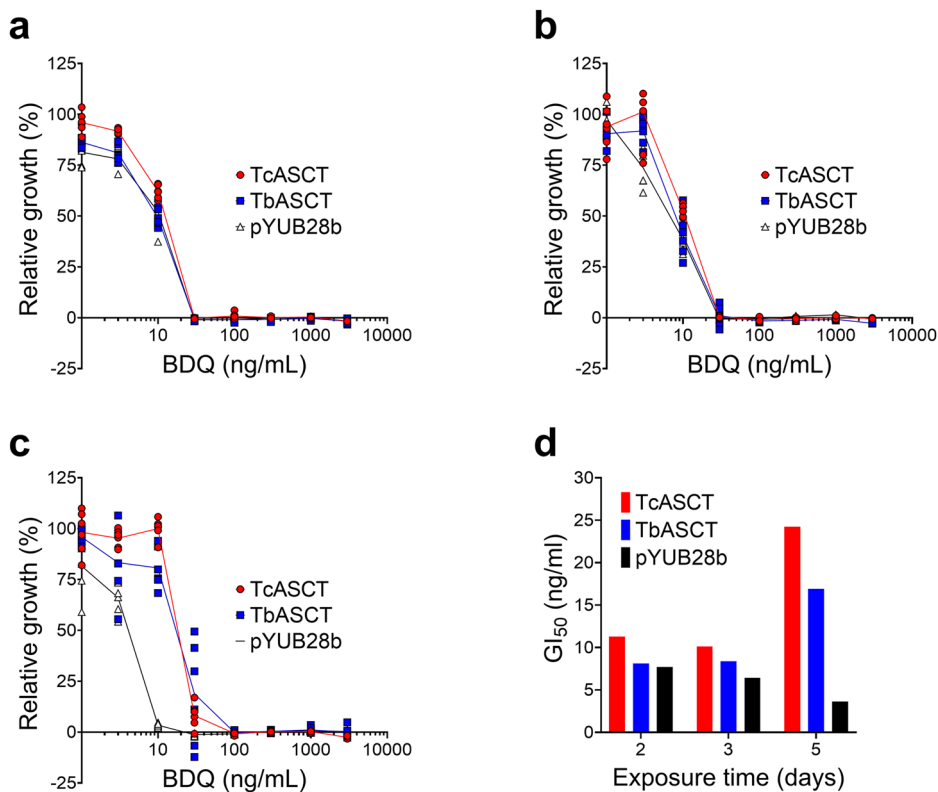
Fig. 6 | Impact of ASCT expression on intracellular ATP levels in *M. smegmatis* exposed to various concentrations of BDQ. Cells were cultured in minimal (HdeB) medium supplemented with 30 mM glycerol and exposed to various concentrations of BDQ. The cultures were incubated at 37 °C with shaking at 200 rpm. At the indicated time points, 1 mL aliquots were collected and assessed for the following: **a** Intracellular ATP levels were determined using the BacTiter-Glo assay kit in the 96-well plates. **b** Simultaneously, growth of the same cells was monitored by measuring the OD$_{600}$. Data are presented as the mean ± SD of two biological replicates.

E. coli[35,36], *Salmonella enterica*[37], and budding yeast[38], ATP synthase has been reported to be non-essential as long as a fermentable carbon source is provided. Since BDQ does not inhibit the ASCT/SCS cycle even at high concentrations (Supplementary Fig. 5), alternative explanations include (i) BDQ may be inhibiting an unidentified pathway (off-target effects), (ii) the

perturbations in several pathways contributing to metabolic poisoning[17], and (iii) the prolonged effect of a hyperpolarized membrane caused by ATP synthase inhibition may be particularly harmful in mycobacteria. Note that inhibition of ATP synthase is expected to lead to the accumulation of acetyl-CoA[17], a condition that could potentially benefit cells expressing ASCT

(Supplementary Fig. 7). While an acetyl-CoA synthethase (ACS) is conserved in *Mycobacterium*[39], it utilizes acetate and CoA as substrates, both of which are products of the ASCT/SCS cycle. However, we do not anticipate a significant increase in ACS levels comparable to ASCT, as it would result in a futile cycle, and consequently, no growth rescue would be observed.

We also found that all transgenic strains of *M. smegmatis* exhibited enhanced growth when cultured in a glucose medium. Additionally, under a glucose-rich medium, the expression of ASCT is beneficial when mycobacteria are exposed to high-concentration BDQ. It has been reported that the ATP provided by SLPHOS (using glucose as a carbon source) is insufficient to overcome the growth inhibition caused by an ATP synthase defect in mycobacteria[22,23]. Notably, the ASCT/SCS cycle supplies two additional ATPs per molecule of glucose consumed[26]. This surplus ATP, exclusive to ASCT-expressing strains and absent in the control (empty vector) strain, holds the potential to effectively counteract the inhibitory effects of low-concentration BDQ on ATP synthase.

We also observed that the effect of BDQ is potentiated in *M. smegmatis* cultured in minimum medium supplemented with glycerol, and the expression of a trypanosomal ASCT provided a better growth rescue rate (ASCT vs. WT strains) compared to when the bacteria were cultured in medium supplemented with other carbon sources (Fig. 4). Note that the initial step of glycerol metabolism in mycobacteria requires one ATP for the synthesis of glycerol-3-phosphate (G3P) by glycerol kinase[40,41], with G3P being oxidized by the menaquinone-dependent G3P dehydrogenase. The produced menaquinol is further oxidized to the proton-motive cytochrome bc_1/aa_3 pathway, resulting in the production of ATP by OXPHOS. In general, inhibition of OXPHOS would cause hyperpolarization of the membrane, resulting in accumulation of menaquinol, unless the electrons from menaquinol are re-routed via the non-proton motive pathways, such as cytochrome *bd*, nitrate reductase and fumarate reductase. Therefore, activation and utilization of glycerol by *M. smegmatis* is strongly dependent on OXPHOS. We conjecture that the additional ATP provided by the ASCT/SCS cycle may facilitate this initial step of glycerol metabolism, with the electrons from G3P being transported by the above-mentioned pathways could explain the enhanced rescue rate for cells growing on glycerol in the presence of low concentrations of BDQ. Taking together, given that the ASCT/SCS cycle is directly involved in ATP synthesis[27,42,43], the expression of ASCT in *M. smegmatis* provides an additional ATP source, leading to increased fitness under BDQ-induced stress, or under ATP-limiting growth conditions.

Methods

Chemicals and reagents
Unless otherwise indicated, all of the commercial reagents employed in this study were obtained from Sigma-Aldrich, Wako, or Promega. Restriction endonuclease enzymes were obtained from New England Biolabs. SCS originating from prokaryotes was acquired from Megazyme (Ireland). BDQ was purchased from Med Chem Express and was formulated at 10 mg/mL in dimethyl sulfoxide (DMSO).

Construction of a plasmid encoding ASCT from *T. cruzi*
The *T. cruzi* ASCT gene (Gene ID: TcCLB.504153.360), without sequences encoding the mitochondrial targeting signal (MTS; deleted for the first 9 codons of the full-length gene; Δ1-9) was amplified by polymerase chain reaction (PCR) using the SUMO-TcASCTΔ[1–9]-F and TcASCT-Rv1 primers and genomic DNA of *T. cruzi* (CL Brener strain) obtained by the DNAZol® reagent according to the manufacturer's protocol as the template. The resulting *asct* gene was inserted into linearised pETSUMO-TOPO vector (Thermo Fisher Scientific) by TA cloning; the ligation mixture was used to transform chemically competent *Escherichia coli* One Shot™ TOP10 (Thermo Fisher Scientific) cells by the heat-shock method. Transformants were selected on Luria-Bertani (LB) agar plates containing 50 μg/mL kanamycin (Kan). Colony PCR was conducted to identify colonies harbouring insert-containing plasmid, which then were inoculated in 5 mL LB medium supplemented with 50 μg/mL Kan. After 16 h, the cells were

harvested, and the plasmid was extracted using a MagExtractor™-Plasmid Kit (TOYOBO), according to the user's manual. The sequence of the *asct* gene insert was confirmed by DNA sequencing (Fasmac Co., Japan) using the cloning primers as well as TcASCT-Fw2, TcASCT-Fw3, and T7-forward and T7-reverse primers. One such plasmid (designated pETSUMO/TcASCT) was used to transform *E. coli* BL21Star™(DE3) competent cells. The resulting strain, designated BL21Star™(DE3)pETSUMO/TcASCT, was stocked in 20% (v/v) glycerol at −80 °C until further use. All primer sequences are provided in Supplementary Table 3.

Plasmid construction for *M. smegmatis* expressing ASCT
The ASCT gene from *T. brucei* (Tb927.11.2690) and *T. cruzi* (TcCLB.504153.360) lacking the sequence encoding the MTS (Δ1-9) were amplified from the pETSUMO/TbASCT[27] (TbASCT_pYUB_F and TbASCT_pYUB_R) and pETSUMO/TcASCT (TcASCT_pYUB_F and TcASCT_pYUB_R) by PCR from genomic DNA using suitable primers (Supplementary Table 3). For each construct, the amplified PCR product was cleaned using a PCR product extraction kit (Toyobo Co., Japan), digested with NcoI and HindIII, and purified with a gel-extraction kit (Toyobo Co., Japan) according to the manufacturer's protocols. The purified inserts for the two genes were ligated (separately) into HindIII-, NcoI-digested pYUB28b, a mycobacterial expression vector that carries the hygromycin (Hyg) resistance gene.

Finally, the ligation mixture was used to transform 100 μL of *E. coli* DH5α competent cells (Thermo Fisher Scientific, USA). Insert-containing colonies were cultured overnight at 200 rpm and 37 °C in 5 mL LB medium containing 100 μg/mL Hyg. Plasmid was extracted from the cells using the MagExtractor™-Plasmid Kit, and sequences were confirmed by DNA sequencing (Fasmac Co.) using the same primers mentioned to make pETSUMO/TcASCT. The plasmid constructs (designated pYUB28b/TbASCT and pYUB28b/TcASCT) with the correct sequences were used to transform *M. smegmatis*.

Western blot analysis
Proteins from the cell lysates were separated using 12% (w/v) SDS–PAGE, then transferred to a polyvinylidene difluoride (PVDF) membrane (Millipore, Billerica, MA, USA). The membrane was blocked in 2% (w/v) BSA (Sigma-Aldrich), followed by overnight incubation at 4 °C with rabbit anti-ASCT antibody (diluted 1:1000 in PBS) as the primary antibody[43]. The membrane then was washed three times with PBS containing Tween® detergent (PBST) and incubated for one hour at room temperature with anti-rabbit immunoglobulin (IgG; Bio-Rad, diluted 1:5000) as the secondary antibody. Bands were visualised using SuperSignal® West Pico Chemiluminescent Substrate (Thermo Fisher Scientific) according to the manufacturer's instructions. Purified recombinant ASCTs[27] were used as controls.

Expression and purification of TcASCT
The glycerol stock of *E. coli* BL21Star™(DE3)pETSUMO/TcASCT was recovered by streaking onto fresh LB agar containing 50 μg/mL Kan, and the plate was incubated overnight at 37 °C. A single colony was inoculated in 360 mL of Terrific Broth medium (pre-culture) and incubated for 15 h at 37 °C. The pre-culture then was used to inoculate six Ultra-Yield™ flasks, each containing 600 mL of Terrific Broth medium (main culture) supplemented with 50 μg/mL Kan and 20 μM of isopropyl β-D-thiogalactopyranose (IPTG), to an initial optical density at 600 nm (OD$_{600}$) of 1.0. These cultures were incubated for 12 h at 20 °C on a rotary shaker (200 rpm, Bioshaker GRB-300, Taitec).

The cultures were harvested by centrifugation for 10 min at 7000×*g*, 4 °C (Rotor R10A, Hitachi CR22N). The cell pellets then were re-suspended to a final volume of 210 mL in Lysis Buffer [50 mM Tris–HCl (pH 8.0), 5 mM imidazole, 20% (v/v) glycerol, 300 mM NaCl, 10 mM MgCl$_2$, 1 mM ethylenediaminetetraacetic acid (EDTA), and 250 μM phenylmethylsulfonyl fluoride (PMSF)]. The cells were lysed by a single passage through a French press (Ohtake) at a constant pressure of 150–180 MPa; lysis was performed at

4 °C. The lysate was centrifuged for 30 min at 30,000×g, 4 °C, to remove the unbroken cells and debris (Rotor R20A2, Hitachi CR22N). The cleared lysate was subjected to ultra-centrifugation for 90 min at 200,000×g, 4 °C (550A rotor, Hitachi CS150FNX). The resulting supernatant corresponded to the cytosolic fraction.

Next, 2 mL of Ni-NTA agarose (QIAGEN), pre-equilibrated in Lysis Buffer, was added to the cytosolic fraction, and the mixture was incubated overnight at 4 °C with constant stirring. The following day, the protein/Ni-NTA mix was loaded into Econo-Pac® chromatography columns (Bio-Rad) and the flow-through was collected. The resin was washed consecutively with 2 mL of Lysis Buffer, 5 mL of Wash Buffer A [50 mM Tris–HCl (pH 8.0), 20 mM imidazole, 20% (v/v) glycerol, 10 mM ATP, 300 mM NaCl, 2.5 mM MgCl$_2$, and 250 μM PMSF], and 30 mL of Wash Buffer B [50 mM Tris–HCl (pH 8.0), 20 mM imidazole, 20% (v/v) glycerol, 300 mM NaCl, 10 mM MgCl$_2$, 1 mM EDTA, and 250 μM PMSF].

TcASCT was eluted by washing the column with 20 mL of Elution Buffer [50 mM Tris–HCl (pH 8.0), 250 mM imidazole, 20% (v/v) glycerol, 300 mM NaCl, 10 mM MgCl$_2$, 1 mM EDTA, and 250 μM PMSF]. The eluate was collected in 1 mL fractions, and the presence of protein (TcASCT) was monitored by measuring the absorbance at 280 nm (A_{280}) using a Nanodrop 2000c (Thermo Fisher Scientific). The fractions with A_{280} values exceeding 2.0 were pooled and concentrated to concentrations exceeding 10 mg/mL using a centrifugal filter device (Amicon® Ultra-15, 30-kDa cutoff; Millipore); the resulting sample was designated the 1st elution.

To decrease the imidazole and NaCl concentration, the concentrated TcASCT protein was diluted 10-fold with Dilution Buffer [50 mM Tris–HCl (pH 8.0), 20% (v/v) glycerol, 150 mM NaCl, 10 mM MgCl$_2$, and 1 mM EDTA]. SUMO protease (Invitrogen) was added to the diluted TcASCT solution at a 1:20 (w/w) protein ratio and digested by incubating at 4 °C overnight.

Pre-equilibrated Ni-NTA agarose (2 mL) was prepared, combined with the protease-digested sample, and incubated for 1 h at 4 °C; the mixture subsequently was loaded onto an Econo-Pac® chromatography column to permit the separation of the tag-free protein from the His6-SUMO tag and the SUMO protease. Purified tag-free TcASCT was collected in the flow-through and concentrated to more than 10 mg/mL using a centrifugal filter device (Amicon® Ultra-15, 30 kDa cutoff). Finally, glycerol was added to a final concentration of 50% (v/v), and this enzyme stock was stored at −30 °C pending further use. The protein concentration was quantified (in duplicate) using the Bio-Rad Assay kit according to the user's manual; bovine serum albumin (BSA; Takara, Japan) was employed as the standard.

The cytosolic, flow-through, wash, elution, and tag-free fractions from each step of the TcASCT purification were subjected to sodium dodecyl sulfate–polyacrylamide gel electrophoresis (SDS–PAGE) according to the method of Laemmli[44]. The stacking and separation gels consisted of 4% and 12% (w/v) acrylamide, respectively. For loading, samples were mixed 1:3 (v/v) with 4×SDS–PAGE loading buffer (240 mM Tris–HCl (pH 6.8), 8% [w/v] SDS, 40% [v/v] glycerol, 0.04% [w/v] bromophenol blue, and 5% [v/v] β-mercaptoethanol] and heated for 5 min at 95 °C. The denatured samples were loaded onto the gel and run alongside the broad-range Precision Plus Protein™ Standard (Bio-Rad for 60 min) at 100 V at room temperature. The gel then was stained with GelCode™ Blue Safe Protein Stain (Thermo Fisher Scientific).

Biochemical characterisation of TcASCT
The optimal temperature for TcASCT activity was determined in a reaction buffer (consisting of 100 mM Tris–HCl (pH 6.8), 1 mM sodium phosphate, 2 mM MgCl$_2$, 0.1% (v/v) Triton X-100, 1 mM ADP, 0.1 mM 5,5′-dithiobis-(2-nitrobenzoic acid) (DTNB), 0.44 U/mL SCS, and 0.5 mM acetyl-CoA) using 10 ng of purified TcASCT per reaction. Reactions were performed in triplicate at temperatures of 20, 25, 30, 35, 37, 40, and 45 °C. The reactions were initiated by the addition of succinate (starting from a 1 M stock solution with pH 7.0) to a final concentration of 10 mM.

The optimal pH for TcASCT activity was determined using a 96-well plate (C96 Maxisorp Nunc-Immuno Plate, Thermo Scientific) assay and a

SpectraMax® Paradigm® Multi-Mode Detection Platform (Molecular Devices); reactions were run at 37 °C in triplicate. Background was recorded for 5 min at 412 nm in 195 μL of reaction mix per well, using 50 mM of each buffer at the various pHs in the reaction mixes, which otherwise consisted of 10 mM sodium phosphate, 2 mM MgCl$_2$, 1 mM ADP, 0.1 mM DTNB, 0.5 mM acetyl-CoA, 0.44 U/mL SCS, and 100 ng/mL TcASCT). Reactions were initiated by the addition of 5 μL of 400 mM succinate. ASCT activity was calculated using the end-point method after 10 min, and the highest activity [in Tris-HCl (pH 7.0)] was defined as 100%.

Routine TcASCT assays were conducted in 1 mL of reaction mixture [100 mM Tris–HCl (pH 7.0), 10 mM sodium phosphate, 2 mM MgCl$_2$, 1 mM ADP, 0.1 mM DTNB, 0.5 mM acetyl-CoA, and 0.44 U/mL SCS] using a black quartz cuvette at 37 °C. After the addition of the enzyme, the background was recorded for 5 min and the reaction was then initiated by the addition of succinate to a final concentration of 20 mM.

The Michaelis constant (K_m) and maximum reaction velocity (V_{max}) values for succinate were determined by measuring TcASCT activity at various succinate concentrations (ranging from 0.2 to 50 mM) at a fixed acetyl-CoA concentration of 0.5 mM. Similarly, the kinetic parameters for acetyl-CoA were determined at various acetyl-CoA concentrations (ranging from 0.005 to 1.0 mM) in the presence of 20 mM succinate. For the substrate inhibition experiment, the V_{max} of succinate was calculated as 198 μmol/min/mg (k_{cat} = 171 s^{-1}) according to the following equation:

$$V = \frac{V_{max} \times [S]}{\left(K_m + [S] \times (1 + [S]/K_i)\right)}$$

where V is velocity, $[S]$ is substrate concentration, and K_i is inhibition constant.

Mycobacterial strain and general culture conditions
The *M. smegmatis* mc^2 4517 strain[45] was provided by Prof. Gregory Cook. Unless otherwise indicated, *M. smegmatis* was grown at 37 °C in LB supplemented with 0.05% (v/v) Tween 80 (LBT) medium or on LBT agar; where appropriate (e.g., for selection of transgenic strains), LBT was supplemented with 50 μg/mL Kan and 100 μg/mL Hyg. To induce the protein expression, 50 μM IPTG was used in all culture medium.

Generation of transgenic *M. smegmatis* expressing ASCT
The mycobacterial expression plasmids were electroporated into *M. smegmatis* mc^2 4517 described previously[45,46]. Briefly, electrocompetent *M. smegmatis* were prepared as follows: Cells were cultured in 10 mL of LBT medium until the OD$_{600}$ reached 0.5. Cells then were harvested by centrifugation for 10 min at 1500×g and 4 °C, washed three times with 10% (v/v) glycerol containing 0.05% (v/v) Tween 80, and resuspended in 40 μL of 10% (v/v) glycerol, 0.05% (v/v) Tween 80. Each aliquot of the freshly prepared electrocompetent cells was mixed with 1 μg of plasmid, transferred directly into a pre-chilled 0.2-cm-gap electroporation cuvette, and electroporated at 2.5 kV, 25 μF, and 1000 Ω using a Bio-Rad Gene Pulser Xcell™. A control strain was generated by transforming cells with the empty vector (pYUB28b alone). Next, LBT (1 mL) was added to each electroporation reaction, and the mixture was transferred to a 15 mL conical tube and incubated for 4 h at 37 °C with rotation. The cells were then plated to LBT agar containing antibiotics, and the plates were incubated for 72 h until colonies were visible.

For each construct, a single colony was used to prepare a primary culture in 10 mL of LBT with antibiotics. Following growth, glycerol was added to 20% (v/v), and the stock was stored frozen at −80 °C pending further use.

Analysis of recombinant strains harbouring trypanosomal ASCTs
A sample of the frozen stock from each primary culture was streaked to LBT agar containing antibiotics and then incubated at 37 °C for 72 h until colonies were visible. A single colony of each construct was used to inoculate a 30 mL preculture of LBT containing antibiotics and 50 μM IPTG. For the

growth experiment, a mid-logarithmic-phase preculture of *M. smegmatis* was diluted to an initial OD_{600} of 0.03 in 50 mL aliquots of LBT, and individual cultures then were exposed to BDQ at various concentrations. Negative controls also were generated by adding an equivalent volume of dimethyl sulfoxide (DMSO), the vehicle used for formulating BDQ. The flasks were incubated with shaking (200 rpm; BR-43FL Bioshaker®) and growth was monitored by measuring the OD_{600} over time.

To assess the effect of carbon source on mycobacterial growth, transgenic mycobacteria were cultured in Hartmans–de-Bont (HdB) minimal medium[47] containing either 22.5 mM malate, 30 mM glycerol, 45 mM acetate, 22.5 mM succinate, or 15 mM glucose as a sole carbon source.

Expression of trypanosomal ASCTs in *M. smegmatis*

M. smegmatis mc[2] 4517 harbouring plasmids encoding either ASCT or the empty plasmid, were grown for 36 h in an LBT medium with antibiotics and IPTG (50 μM). The cultures then were centrifuged (10 min, 8000×*g*, 4 °C); the resulting pellets were washed three times with ice-cold phosphate-buffered saline (PBS), then resuspended in 5 mL of 50 mM Tris–HCl (pH 7.4) in which complete mini EDTA-free protease-inhibitor tablets (Roche, Germany) had been dissolved. Cells were disrupted by sonication, as described previously[48,49]. After sonication, unbroken cells and debris were removed by centrifugation for 30 min at 10,000×*g*, 4 °C. The cleared mycobacterial cell lysates were then used for protein quantification, western blot analysis, and measurement of specific activity. The protein concentration was quantified (in duplicate) using the Bio-Rad Assay kit according to the user's manual; BSA was employed as the standard.

Activity of trypanosomal ASCTs expressed in *M. smegmatis*

To determine the activity of ASCT expressed in *M. smegmatis*, mycobacterial lysates were assayed by quantifying CoA release, as detected using DTNB[27]. Briefly, ASCT activity was evaluated using the mycobacterial lysates in a 1 mL assay mix consisting of 100 mM Tris–HCl (pH 7.0), 10 mM sodium phosphate (pH 7.2), 2 mM $MgCl_2$, 1 mM ADP, 0.1 mM DTNB, 0.5 mM acetyl-CoA and 0.44 U/mL SCS. The mixture was pre-warmed to 37 °C and the reaction was initiated by the addition of succinate to a final concentration of 20 mM; the production of CoA was monitored spectrophotometrically (V760, Jasco Co., Japan) at 412 nm. The specific activity was calculated based on the extinction coefficient of 2-nitro-5-thiobenzoate ($14.0\ mM^{-1}\ cm^{-1}$).

Growth inhibition assay (GI_{50} determination)

Susceptibility of mycobacterial strains to BDQ was quantified using a previously described resazurin microtiter assay (REMA)[50]. Briefly, *M. smegmatis* cultured overnight in LBT medium containing antibiotics and IPTG was diluted into a fresh medium to an OD_{600} of 0.05 and a total volume of 100 μL was distributed to the wells of a 96-well plate. Serial ten-fold dilutions of BDQ (at concentrations ranging from 3 μg/mL to 1 ng/mL) were added to the wells, and the plates were incubated at 37 °C with mild shaking (75 rpm). Wells of cells exposed to DMSO (the vehicle for BDQ) or containing medium only (no cells) were included as controls. At the indicated time points, 30 μL of 0.2 mg/mL resazurin was added to each well, and the plates were incubated for an additional 6 h at 37 °C. Fluorescence in the individual wells then was measured using a SpectraMax® Paradigm® plate reader at excitation and emission wavelengths of 560 and 590 nm, respectively. The concentration of the compound that inhibits cell growth to 50% (GI_{50}) was calculated by applying the log (inhibitor) versus a normalised response-variable slope equation (Hill equation) in the Prism software package (v 8.4.3; GraphPad, San Diego, CA, USA).

Measurement of intracellular ATP levels

To quantify intracellular ATP levels, the BacTiter-Glo™ Microbial Cell Viability Assay Kit (Promega) was used according to the manufacturer's instructions, as previously described[51]. Briefly, transgenic mycobacterial strains were cultured in 100 mL of minimal medium in a 500 mL baffled flask. The medium contained antibiotics, IPTG, and 30 mM glycerol (v/v).

The cultures were exposed to various concentrations of BDQ. At each time, a 1 mL aliquot from each culture was collected to measure growth (OD_{600}). Additionally, 25 μL of the same sample was mixed with 75 μL of cold PBS, making a total volume of 100 μL. This mixture was then transferred to a well of a 96-well white plate. An equal volume of BacTiter-Glo reagent was added to each well, the contents were mixed, and the plates were incubated for 10 min in the dark at room temperature. The luminescence of each well was recorded using the SpectraMax® Paradigm® plate reader and expressed as relative light units (RLU). ATP standards (0.1–100 nM) were included as an internal control.

Statistics and reproducibility

Descriptive statistics (mean, standard deviation, standard error) and GI_{50} values were determined using Prism. Inferential statistical analyses were conducted using two-tailed one-way ANOVA with post hoc Tukey's tests. $p < 0.05$ was considered statistically significant.

Data availability

All data behind the graphs and tables in this paper are presented in the Supplementary Data 1 and 2 files. Detailed information supporting the results and conclusions of this paper is available upon reasonable request from the corresponding author.

References

1. WHO. *Global Tuberculosis Report 2022 Factsheet* (World Health Organization, 2022).
2. WHO. *Global Tuberculosis Report 2021* (World Health Organization, Geneva, Switzerland; 2021).
3. Koul, A., Arnoult, E., Lounis, N., Guillemont, J. & Andries, K. The challenge of new drug discovery for tuberculosis. *Nature* **469**, 483–490 (2011).
4. Ma, Z., Lienhardt, C., McIlleron, H., Nunn, A. J. & Wang, X. Global tuberculosis drug development pipeline: the need and the reality. *Lancet* **375**, 2100–2109 (2010).
5. Cook, G. M. et al. Oxidative phosphorylation as a target space for tuberculosis: success, caution, and future directions. *Microbiol. Spectr.* **5**, https://doi.org/10.1128/microbiolspec.tbtb2-0014-2016 (2017).
6. Cook, G. M., Hards, K., Vilcheze, C., Hartman, T. & Berney, M. Energetics of respiration and oxidative phosphorylation in mycobacteria. *Microbiol. Spectr.* **2**, https://doi.org/10.1128/microbiolspec.MGM2-0015-2013 (2014).
7. Lu, P., Lill, H. & Bald, D. ATP synthase in mycobacteria: special features and implications for a function as drug target. *Biochim. Biophys. Acta* **1837**, 1208–1218 (2014).
8. Koul, A. et al. Diarylquinolines are bactericidal for dormant mycobacteria as a result of disturbed ATP homeostasis. *J. Biol. Chem.* **283**, 25273–25280 (2008).
9. Lu, P. et al. The anti-mycobacterial activity of the cytochrome *bcc* inhibitor Q203 can be enhanced by small-molecule inhibition of cytochrome *bd*. *Sci. Rep.* **8**, 2625 (2018).
10. Andries, K. et al. A diarylquinoline drug active on the ATP synthase of *Mycobacterium tuberculosis*. *Science* **307**, 223–227 (2005).
11. Bald, D. & Koul, A. Respiratory ATP synthesis: the new generation of mycobacterial drug targets? *FEMS Microbiol. Lett.* **308**, 1–7 (2010).
12. Lelovic, N. et al. Application of *Mycobacterium smegmatis* as a surrogate to evaluate drug leads against *Mycobacterium tuberculosis*. *J. Antibiot. (Tokyo)* **73**, 780–789 (2020).
13. Chaturvedi, V., Dwivedi, N., Tripathi, R. P. & Sinha, S. Evaluation of *Mycobacterium smegmatis* as a possible surrogate screen for selecting molecules active against multi-drug resistant *Mycobacterium tuberculosis*. *J. Gen. Appl. Microbiol.* **53**, 333–337 (2007).

14. Hards, K. et al. Bactericidal mode of action of bedaquiline. *J. Antimicrob. Chemother.* **70**, 2028–2037 (2015).

15. Hards, K. et al. Ionophoric effects of the antitubercular drug bedaquiline. *Proc. Natl Acad. Sci. USA* **115**, 7326–7331 (2018).

16. Koul, A. et al. Diarylquinolines target subunit c of mycobacterial ATP synthase. *Nat. Chem. Biol.* **3**, 323–324 (2007).

17. Mackenzie, J. S. et al. Bedaquiline reprograms central metabolism to reveal glycolytic vulnerability in *Mycobacterium tuberculosis*. *Nat. Commun.* **11**, 6092 (2020).

18. Koul, A. et al. Delayed bactericidal response of *Mycobacterium tuberculosis* to bedaquiline involves remodelling of bacterial metabolism. *Nat. Commun.* **5**, 3369 (2014).

19. Andries, K. et al. Acquired resistance of *Mycobacterium tuberculosis* to bedaquiline. *PLoS ONE* **9**, e102135 (2014).

20. Andres, S. et al. Bedaquiline-resistant tuberculosis: dark clouds on the horizon. *Am. J. Respir. Crit. Care Med.* **201**, 1564–1568 (2020).

21. Lamprecht, D. A. et al. Turning the respiratory flexibility of *Mycobacterium tuberculosis* against itself. *Nat. Commun.* **7**, 12393 (2016).

22. Sassetti, C. M., Boyd, D. H. & Rubin, E. J. Genes required for mycobacterial growth defined by high density mutagenesis. *Mol. Microbiol.* **48**, 77–84 (2003).

23. Tran, S. L. & Cook, G. M. The F1Fo-ATP synthase of *Mycobacterium smegmatis* is essential for growth. *J. Bacteriol.* **187**, 5023–5028 (2005).

24. Van Hellemond, J. J., Opperdoes, F. R. & Tielens, A. G. Trypanosomatidae produce acetate via a mitochondrial acetate: succinate CoA transferase. *Proc. Natl Acad. Sci. USA* **95**, 3036–3041 (1998).

25. Tielens, A. G., van Grinsven, K. W., Henze, K., van Hellemond, J. J. & Martin, W. Acetate formation in the energy metabolism of parasitic helminths and protists. *Int. J. Parasitol.* **40**, 387–397 (2010).

26. Millerioux, Y. et al. ATP synthesis-coupled and -uncoupled acetate production from acetyl-CoA by mitochondrial acetate:succinate CoA-transferase and acetyl-CoA thioesterase in *Trypanosoma*. *J. Biol. Chem.* **287**, 17186–17197 (2012).

27. Mochizuki, K. et al. The ASCT/SCS cycle fuels mitochondrial ATP and acetate production in *Trypanosoma brucei*. *Biochim. Biophys. Acta Bioenerg.* **1861**, 148283 (2020).

28. Bashiri, G., Rehan, A. M., Greenwood, D. R., Dickson, J. M. & Baker, E. N. Metabolic engineering of cofactor F420 production in *Mycobacterium smegmatis*. *PLoS ONE* **5**, e15803 (2010).

29. Kalia, N. P. et al. Carbon metabolism modulates the efficacy of drugs targeting the cytochrome *bc*1:*aa*3 in *Mycobacterium tuberculosis*. *Sci. Rep.* **9**, 8608 (2019).

30. Danelishvili, L. et al. *Mycobacterium tuberculosis* proteome response to antituberculosis compounds reveals metabolic "escape" pathways that prolong bacterial survival. *Antimicrob. Agents Chemother.* **61**, e00430-17 (2017).

31. Villellas, C. et al. Unexpected high prevalence of resistance-associated Rv0678 variants in MDR-TB patients without documented prior use of clofazimine or bedaquiline. *J. Antimicrob. Chemother.* **72**, 684–690 (2017).

32. Almeida, D. et al. Mutations in pepQ Confer low-level resistance to bedaquiline and clofazimine in *Mycobacterium tuberculosis*. *Antimicrob. Agents Chemother.* **60**, 4590–4599 (2016).

33. Gengenbacher, M., Rao, S. P. S., Pethe, K. & Dick, T. Nutrient-starved, non-replicating *Mycobacterium tuberculosis* requires respiration, ATP synthase and isocitrate lyase for maintenance of ATP homeostasis and viability. *Microbiology (Reading)* **156**, 81–87 (2010).

34. Frampton, R., Aggio, R. B., Villas-Boas, S. G., Arcus, V. L. & Cook, G. M. Toxin-antitoxin systems of *Mycobacterium smegmatis* are essential for cell survival. *J. Biol. Chem.* **287**, 5340–5356 (2012).

35. Friedl, P. et al. Membrane integration and function of the three F0 subunits of the ATP synthase of *Escherichia coli* K12. *EMBO J.* **2**, 99–103 (1983).

36. Wang, Z., Hicks, D. B., Guffanti, A. A., Baldwin, K. & Krulwich, T. A. Replacement of amino acid sequence features of a- and c-subunits of ATP synthases of Alkaliphilic *Bacillus* with the *Bacillus* consensus sequence results in defective oxidative phosphorylation and non-fermentative growth at pH 10.5. *J. Biol. Chem.* **279**, 26546–26554 (2004).

37. Braetz, S., Schwerk, P., Thompson, A., Tedin, K. & Fulde, M. *Salmonella* central carbon metabolism enhances bactericidal killing by fluoroquinolone antibiotics. *Antimicrob. Agents Chemother.* **66**, e0234421 (2022).

38. Malecki, M., Kamrad, S., Ralser, M. & Bahler, J. Mitochondrial respiration is required to provide amino acids during fermentative proliferation of fission yeast. *EMBO Rep.* **21**, e50845 (2020).

39. Noy, T., Xu, H. & Blanchard, J. S. Acetylation of acetyl-CoA synthetase from *Mycobacterium tuberculosis* leads to specific inactivation of the adenylation reaction. *Arch. Biochem. Biophys.* **550–551**, 42–49 (2014).

40. Blotz, C. & Stulke, J. Glycerol metabolism and its implication in virulence in *Mycoplasma*. *FEMS Microbiol. Rev.* **41**, 640–652 (2017).

41. Hunter, G. J. The oxidation of glycerol by Mycobacteria. *Biochem. J.* **55**, 320–328 (1953).

42. Rucker, N. et al. Acetate dissimilation and assimilation in *Mycobacterium tuberculosis* depend on carbon availability. *J. Bacteriol.* **197**, 3182–3190 (2015).

43. Riviere, L. et al. Acetyl:succinate CoA-transferase in procyclic *Trypanosoma brucei*. Gene identification and role in carbohydrate metabolism. *J. Biol. Chem.* **279**, 45337–45346 (2004).

44. Laemmli, U. K. Cleavage of structural proteins during the assembly of the head of bacteriophage T4. *Nature* **227**, 680–685 (1970).

45. Wang, F. et al. *Mycobacterium tuberculosis* dihydrofolate reductase is not a target relevant to the antitubercular activity of isoniazid. *Antimicrob. Agents Chemother.* **54**, 3776–3782 (2010).

46. Snapper, S. B. et al. Isolation and characterization of efficient plasmid transformation mutants of *Mycobacterium smegmatis*. *Mol. Microbiol.* **4**, 1911–1919 (1990).

47. Song, H. & Niederweis, M. Uptake of sulfate but not phosphate by *Mycobacterium tuberculosis* is slower than that for *Mycobacterium smegmatis*. *J. Bacteriol.* **194**, 956–964 (2012).

48. Gajadeera, C. et al. Antimycobacterial activity of DNA intercalator inhibitors of *Mycobacterium tuberculosis* primase DnaG. *J. Antibiot. (Tokyo)* **68**, 153–157 (2015).

49. Rabodoarivelo, M. S. et al. Optimizing of a protein extraction method for *Mycobacterium tuberculosis* proteome analysis using mass spectrometry. *J. Microbiol. Methods* **131**, 144–147 (2016).

50. Agrawal, P., Miryala, S. & Varshney, U. Use of *Mycobacterium smegmatis* deficient in ADP-ribosyltransferase as surrogate for *Mycobacterium tuberculosis* in drug testing and mutation analysis. *PLoS ONE* **10**, e0122076 (2015).

51. Vargas-Blanco, D. A., Zhou, Y., Zamalloa, L. G., Antonelli, T. & Shell, S. S. mRNA degradation rates are coupled to metabolic status in *Mycobacterium smegmatis*. *mBio* **10**, e00957-19 (2019).

Acknowledgements

Author contributions

Experiment concept and design: D.K.I., Y.M., G.M.C., G.M.B., F.B., M.B., K.K. and K.H. Conduct of experiments: G.M.B., K.M., Y.A. and A.R. Analysis of data: G.M.B., K.M., D.K.I., G.M.C., M.H., T.S., S.H. and M.S. Formalisation of the paper: G.M.B. and D.K.I. All authors have read and approved the final version of the manuscript.

Competing interests

The authors declare no competing interests.

Additional information

Supplementary information The online version contains supplementary material available at https://doi.org/10.1038/s42003-025-07611-0.

Correspondence and requests for materials should be addressed to Daniel Ken Inaoka.

Peer review information *Communications Biology* thanks Pieter Steketee and the other, anonymous, reviewer(s) for their contribution to the peer review of this work. Primary Handling Editors: Karthika Rajeeve and Tobias Goris.

Reprints and permissions information is available at http://www.nature.com/reprints

Publisher's note Springer Nature remains neutral with regard to jurisdictional claims in published maps and institutional affiliations.

[1]Program for Nurturing Global Leaders in Tropical and Emerging Communicable Disease, Graduate School of Biomedical Sciences, Nagasaki University, Nagasaki, Japan. [2]Department of Parasitology, Institute of Tropical Medicine (NEKKEN), Nagasaki University, Nagasaki, Japan. [3]Department of Molecular Infection Dynamics, Institute of Tropical Medicine (NEKKEN), Nagasaki University, Nagasaki, Japan. [4]Department of Immunogenetics, Institute of Tropical Medicine (NEKKEN), Nagasaki University, Nagasaki, Japan. [5]Department of Paediatrics, Kinshasa University Hospital, University of Kinshasa, Kinshasa, Democratic Republic of Congo. [6]Department of Medical Zoology, Kanazawa Medical University, Ishikawa, Japan. [7]School of Tropical Medicine and Global Health, Nagasaki University, Nagasaki, Japan. [8]Graduate School of Life Science, Kumamoto University, Kumamoto, Japan. [9]Department of Infection Biochemistry, Institute of Tropical Medicine (NEKKEN), Nagasaki University, Nagasaki, Japan. [10]Department of Infectious Disease Control, Oita University, Oita, Japan. [11]Department of Microbiology and Immunology, University of Otago, Dunedin, New Zealand. [12]Maurice Wilkins Centre for Molecular Biodiscovery, University of Auckland, Auckland, New Zealand. [13]Laboratoire de Microbiologie Fondamentale et Pathogénicité (MFP), Université de Bordeaux, Bordeaux, France. [14]Fakultät für Biologie, Genetik, Ludwig-Maximilians-Universität München, München, Germany. [15]Department of Computer Science, Institute of Science Tokyo, Tokyo, Japan. [16]Department of Biomedical Chemistry, Graduate School of Medicine, The University of Tokyo, Tokyo, Japan. ✉e-mail: danielken@nagasaki-u.ac.jp